ISSN 0001-4338, Izvestiya, Atmospheric and Oceanic Physics, 2015, Vol. 51, No. 1, pp. 89–97. © Pleiades Publishing, Ltd., 2015.
Original Russian Text © T.G. Talipova, O.E. Kurkina, E.A. Rouvinskaya, E.N. Pelinovsky, 2015, published in Izvestiya AN. Fizika Atmosfery i Okeana, 2015, Vol. 51, No. 1, pp. 103–112.

Propagation of Solitary Internal Waves in Two-Layer Ocean of Variable Depth

T. G. Talipova[a, b], O. E. Kurkina[b, c], E. A. Rouvinskaya[b], and E. N. Pelinovsky[a, b, c]

[a] *Institute of Applied Physics, Russian Academy of Sciences, ul. Ul'yanova 46, Nizhny Novgorod, 603950 Russia*
e-mails: tgtalipova@mail.ru, pelinovsky@gmail.com
[b] *Nizhni Novgorod State Technical University, ul. Minina 24, Nizhni Novgorod, 603950 Russia*
[c] *Higher School of Economics National Research University, ul. Bol'shaya Pecherskaya 25/12, Nizhni Novgorod, 603155 Russia*

Received September 6, 2013; in final form October 9, 2013

Abstract—The propagation of internal solitons of moderate amplitude in a two-layer ocean of variable depth is studied in terms of the Gardner and Euler equations. An analytical solution is obtained with the use of asymptotic expansions on a small parameter (bottom slope). The theoretical results are compared with the numerical modeling results. The possibility of soliton shape preservation during pulse propagation is discussed. It is obtained that, as the initial amplitude increases, the pulse deviates from the soliton shape more rapidly.

Keywords: internal waves, two-layer ocean, Euler equations, Gardner equation, soliton

DOI: 10.1134/S0001433815010107

INTRODUCTION

In the last decades, a change in polarity of solitary internal waves (solitons) has been observed very often in the coastal zones. In particular, this phenomenon was reported in the Eastern Mediterranean [1], the northwestern shelf of Australia [2], the South China Sea (during the ASIAEX experiment) [3–11], the New Jersey [12] and St. Lawrence [14] bays, the shelf of Kamchatka [15], and in other places as well. This phenomenon is caused by a change in sign of the internal-wave quadratic nonlinearity due to both lateral variation in density stratification and decreasing depth during wave propagation towards the shore. A change in sign of soliton has been repeatedly modeled in terms of nonlinear evolutionary equations of Korteweg–de Vries type and its generalizations from different regions of the World Ocean [2, 5, 16–18]. Numerical modeling in terms of the Euler equations also verifies the change in soliton polarity, for example, in the Andaman Sea [19] and Konstanz Lake [20], and provides a good fit with the observations in St. Lawrence Bay [14].

In theory, beyond the zone of change in quadratic nonlinearity sign, the adiabatic transformation of internal wave soliton is usually considered when the ocean parameters change in such a gentle manner that soliton preserves its shape in every moment of time; only its amplitude and length change. The reconstruction of internal wave soliton in different shelf zones of the World Ocean is studied in terms of the Gardner equation [17, 18, 21–23]; this allows researchers to find the relationship between soliton amplitude and the local medium parameters. The calculations show that adiabatic transformation of soliton can take place within considerable areas of shelf zones, where nonlinearity does not change sign and the change in medium parameters is quite gentle [17, 18]. The numerical integration of nonlinear Euler equations for internal waves in the shelf zone of Oregon, in the framework of the CODE experiment, is also an example of the adiabatic propagation of soliton [24].

A detailed analysis of how soliton polarity changes when changing only the sign of quadratic nonlinearity has been made in [21, 22, 25, 26]; that when changing only the sign of cubic nonlinearity was made in [27]. In these publications, the area where soliton loses its shape due to a change in nonlinearity sign has been shown, as well as the further transformation of soliton not in accord with the adiabatic theory.

However, the gentle character of change in medium parameters and distances to the points where the nonlinearity sign changes is a necessary, though not sufficient, condition of adiabatic propagation of solitons. In the present work, the transformation of the internal wave soliton in a two-layer ocean of linearly and gently changing depth is studied in detail. Analytical results obtained by the asymptotic theory are compared to those obtained numerically by the Gardner and Euler equations. The aim of this analysis is to clarify the range of applicability for the asymptotic model and determine the additional conditions for the adiabatic transformation of soliton. The theory of adia-

batic transformation of soliton in an inhomogeneous ocean is described in Section 1. The data of numerical calculations are given in Section 2. The results are summarized in the Conclusions. The numerical models are presented in the Appendix.

1. ADIABATIC APPROXIMATION OF THE GARDNER EQUATION IN A HORIZONTALLY INHOMOGENEOUS MEDIUM

The dynamics of long nonlinear internal waves of moderate amplitude in a two-layer ocean of variable depth is described by the generalized Gardner equation [1, 16, 28]

$$\frac{\partial\xi}{\partial x}+\left(\frac{\alpha(x)Q(x)}{c^2(x)}\xi+\frac{\alpha_1(x)Q^2(x)}{c^2(x)}\xi^2\right)\frac{\partial\xi}{\partial s}+\frac{\beta(x)}{c^4(x)}\frac{\partial^3\xi}{\partial s^3}=0. \quad (1)$$

This equation is written for the modified shift of the interface between the ocean layers

$$\xi(s,x)=\frac{\eta(s,x)}{Q(x)},$$

where η is the shift of the interface between the layers. The other parameters of Eq. (1) are set by the following analytical expressions:

$$c(x)=\sqrt{\frac{g\Delta\rho}{\rho}\frac{h_1h_2(x)}{h_1+h_2(x)}},\quad s=\int\frac{dx}{c(x)}-t,$$
$$\alpha(x)=\frac{3c}{2}\frac{h_1-h_2(x)}{h_1h_2(x)},\quad \beta(x)=\frac{ch_1h_2(x)}{6},$$
$$\alpha_1(x)=-\frac{3c}{8h_1^2h_2^2(x)}\left(h_1^2+h_2^2(x)+6h_1h_2(x)\right),$$
$$Q(x)=\left(\frac{h_{20}}{h_1}\frac{h_1+h_2(x)}{h_1+h_{20}}\right)^{1/4}.$$

Zero in the right part of Eq. (1) means the initial point from which the wave propagates. The upper layer has the constant thickness h_1, while the lower one has variable depth $h_2(x)$; $\Delta\rho/\rho$ is the density surge at the interface between the layers and g is the free-fall acceleration.

As is clearly seen, the coefficient of quadratic nonlinearity α changes its sign in the point where the thicknesses of two layers become equal, while the coefficient of cubic nonlinearity α_1 is always negative. Note that the Gardner equation (1) with variable coefficients is not integrable, but has two important conservation integrals: the one of mass flow

$$\int_{-\infty}^{+\infty}\xi(s,x)ds=\int_{-\infty}^{+\infty}\xi(t,x)dt=\int_{-\infty}^{+\infty}\eta(t,0)dt \quad (2)$$

and the one of energy flow

$$\int_{-\infty}^{+\infty}\xi^2(s,x)ds=\int_{-\infty}^{+\infty}\xi^2(t,x)dt=\int_{-\infty}^{+\infty}\eta^2(t,0)dt. \quad (3)$$

In the case when ocean depth changes slowly, the soliton can be described, in the first approximation, by the expression

$$\xi_s=\frac{A}{1+B\mathrm{ch}\left[\gamma\left(s-\kappa x\right)\right]}, \quad (4)$$

where A, B, κ, and γ are interrelated parameters

$$A=\frac{6\beta\gamma^2}{Q\alpha c^2},\quad \gamma=\sqrt{\frac{\alpha^2c^2}{6\alpha_1\beta}(B^2-1)},\quad \kappa=\frac{\beta\gamma^2}{c^4}. \quad (5)$$

The amplitude a of soliton is found as follows

$$a=\frac{QA}{(1+B)}=\frac{Q\alpha}{\alpha_1}(B-1). \quad (6)$$

The shape of soliton found from Eq. (4) depends on the sole parameter (amplitude): at small amplitudes, the shape of soliton is closer to that by the Korteweg–de Vries equation, while at high ones ($B\to 0$) soliton tends to the limiting, so called "thick," soliton, whose amplitude is found as follows:

$$A_{lim}=-\frac{Q\alpha}{\alpha_1}. \quad (7)$$

Here, the parameters of soliton depend on local depth, while amplitude is arbitrary. The change in amplitude of soliton with depth can be found analytically using the law of energy flow preservation from Eq. (3) [17, 29].

$$E(x)=\frac{1}{Q^2c}\sqrt{\frac{\alpha^2\beta}{|\alpha_1^3|}}\left(2\mathrm{arccoth}\sqrt{\frac{1-B}{1+B}}-\sqrt{1-B^2}\right)=E(x_0),$$

From whence we obtain the following transcendent equation relative to the parameter $B(x)$ directly connected with the amplitude of wave from Eq. (6):

$$\sqrt{\frac{(\alpha(x))^2\beta(x)}{|(\alpha_1(x))^3|}}\frac{1}{(Q(x_0,x))^2c(x)}\times\left(2\mathrm{arccoth}\left(\sqrt{\frac{1-B(x)}{1+B(x)}}\right)-\sqrt{1-(B(x))^2}\right)$$
$$=\sqrt{\frac{(\alpha(x_0))^2\beta(x_0)}{|(\alpha_1(x_0))^3|}}\frac{1}{(Q(x_0,x_0))^2c(x_0)}\times\left(2\mathrm{arccoth}\left(\sqrt{\frac{1-B(x_0)}{1+B(x_0)}}\right)-\sqrt{1-(B(x_0))^2}\right). \quad (8)$$

Hence, we can find the value of amplitude of soliton in any point x. Note that, for the Korteweg–de Vries equation (small amplitudes), the width γ of soliton from Eq. (5) tends to infinity at an amplitude tending

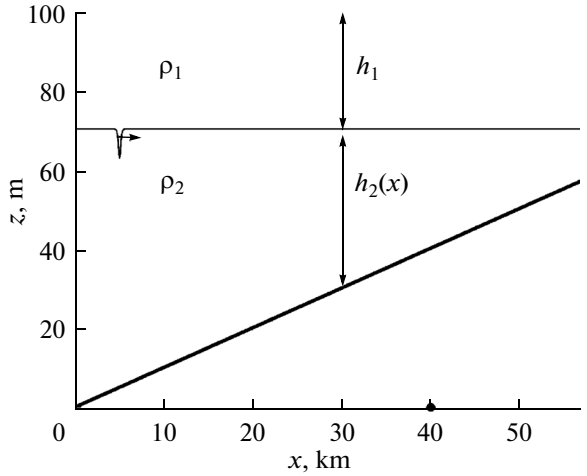

Fig. 1. Scheme of the problem.

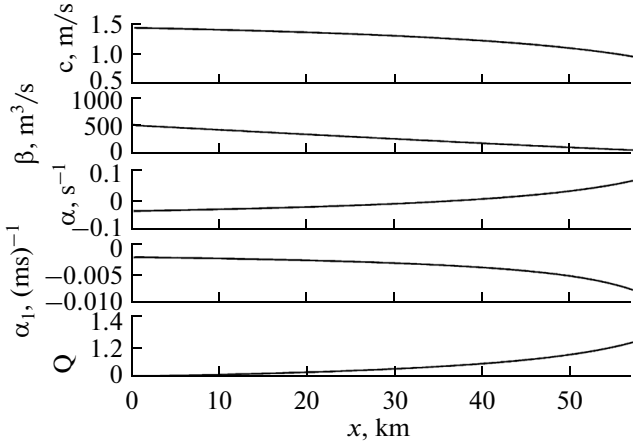

Fig. 2. Change in coefficients of the model with distance.

to zero. As amplitude grows, the soliton becomes more of a "Gardner type," and its width first decreases and then increases and tends to infinity at the amplitude of thick soliton tending to the limiting amplitude (13). Now it is clear that, in extreme cases of small and big amplitudes, when the soliton width is big, the asymptotic theory should not work. The condition for applicability of the asymptotic theory is small width of soliton (in fact, small length of nonlinearity) when compared to the characteristic change in depth.

To construct concrete dependences, let us consider the transformation of long solitary waves of moderate amplitude in the concrete numerical chute with two-layer stratification and gently sloping bottom (Fig. 1). The length of the sloped part of the chute is 57 km; total depth of the basin changes from $H_0 = 100$ m to $H_1 = 43$ m; bottom slope $k = 0.001$; the interface between two layers of liquid (picnocline) is located at the depth $h_1 = 30$ m from the surface. The density surge $\Delta\rho/\rho$ is 0.01. The turning point is where the coefficient of quadratic nonlinearity becomes zero (at a distance of 40 km, where total depth is 60 m). At big depths, the coefficient of quadratic nonlinearity is negative, while it is positive at small ones.

The dependence of coefficients in Eq. (1) on the coordinate is shown in Fig. 2. All coefficients change quite smoothly and monotonously. The dependence of width of the "Gardner type" soliton on the amplitude of the same soliton is shown in Fig. 3. The points indicate the ratios between length and amplitude of the solitons, whose dynamics is modeled in the present work. For the chosen solitons ($a = 3.3$ m, $\lambda = 403.2$ m; $a = 7.3$ m, $\lambda = 311.2$ m; $a = 9.7$ m, $\lambda = 298.6$ m; $a = 12.9$ m, $\lambda = 309.2$ m; $a = 17.5$ m, $\lambda = 453.6$ m), the family of curves was constructed in terms of adiabatic theory (8). These curves describe the dependence of dimensionless amplitude a/a_0 (the ratio between amplitude of reconstructing soliton in the point x and that of the initial soliton) on the distance x to the turning point (Fig. 4).

Note that the lengths of the chosen initial solitons are no more than one percent of the distance to the turning point (i.e., the adiabatic theory is applicable in this case).

As was noticed in [22], where only the change in coefficient of quadratic nonlinearity with distance was considered, the amplitude of nearly limiting soliton, in terms of the adiabatic theory, decreases with distance almost following the linear law, while soliton constantly remains limiting. Such a behavior for amplitude of limiting soliton is also observed when all coefficients of the Gardner equation change during the propagation of soliton (Fig. 4, curve *5*).

Solitons with small initial amplitude (Fig. 4, curves *1* and *2*) behave first as those of the "Korteweg–de Vries type," but their shape approach the limiting one as depth decreases and then amplitude decreases linearly.

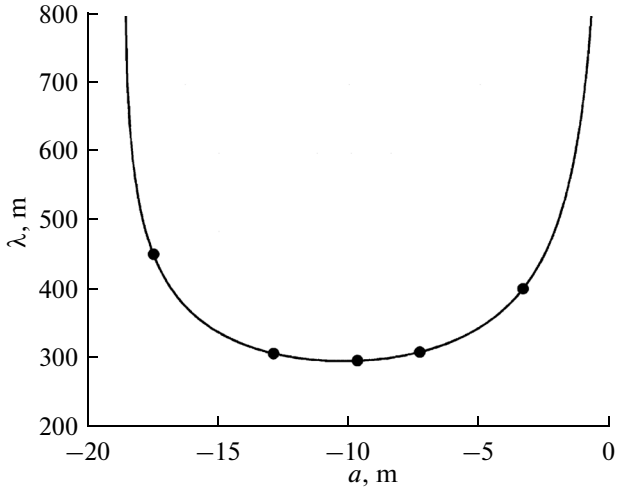

Fig. 3. Curve showing the dependence of width of the Gardner soliton on amplitude of the same soliton.

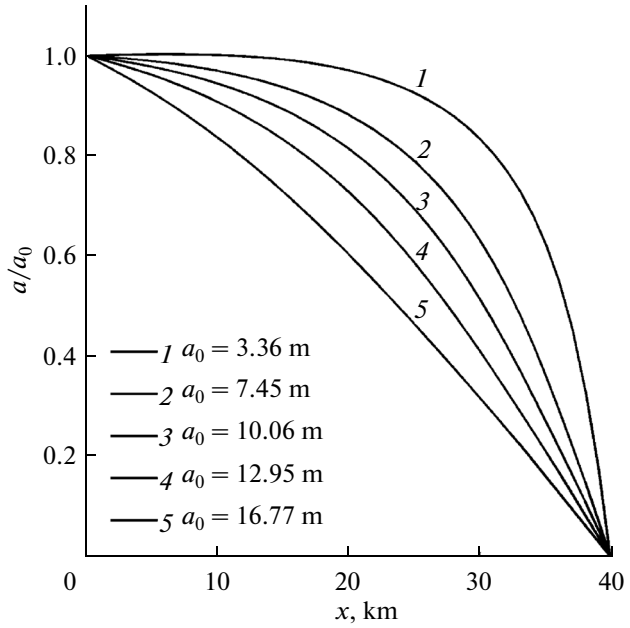

Fig. 4. Dependence of dimensionless amplitude a/a_0 on distance x in terms of the adiabatic theory.

Obviously, as the point of zero nonlinearity is approached, the width of soliton in the adiabatic theory grows with no limit and, beginning at a particular moment, adiabatic theory becomes inapplicable in principle.

Qualitatively, the change in amplitude of soliton in terms of the adiabatic theory in a situation, when all the parameters of model equation (1) change, is very similar to the change in amplitude when the only changing parameter is that of quadratic nonlinearity [22]. Note that it is the parameter of quadratic nonlinearity that determines soliton behavior when approaching the turning point.

Below, the limits of applicability for the adiabatic theory are estimated on the basis of a comparison between the results of numerically modeling soliton propagation in terms of both the Gardner asymptotic equation and the Euler equations.

2. RESULTS OF NUMERICAL MODELING

Numerical modeling was implemented for the conditions described above. When the initial solitonlike pulses (Gardner equation solitons) were set in terms of the Euler equations, the sloped bottom was joined to the flat bottom site at which the initial pulse had been set. The initial amplitudes of solitonlike pulses were also chosen in accord with solitons mentioned above (−3.3, −7.3, −9.7, −12.9, and −17.5 m). The biggest width of the initial pulse was about 453.6 m, which is much less than the scale of medium inhomogeneity (1.1% of the distance to the turning point). Transformation of solitons was also modeled in terms of the numerical model based on the Gardner equation. Figure 5 exhibits the results of modeling solitons with initial amplitudes of −3.3, −9.7, and −17.5 m (in terms of both models). Here, the solid line indicates the transformation of the initial soliton calculated by the Gardner equation; the dashed line indicates the same transformation in terms of the Euler full-nonlinear model. In Gardner equation (1), coordinate x is the evolutionary variable and the pulse calculated by the evolutionary model is shown on the time scale located on top, in the points x, whose values are indicated below the x axis. In the full-nonlinear model, in the same points x, the time record of wave is drawn (also seen in the figure). For illustrative purposes, the thick solid line indicates the bottom position relative to the x axis.

In all three cases, a wave moves faster in the Gardner model than in the full-nonlinear one, as was reported in [30, 31].

The higher the amplitude of the initial soliton is, the earlier the soliton shape is lost; soliton generates a positive "step" before the turning point (40 km) in terms of both numerical models. This "step" is higher in the Gardner model than in the full-nonlinear one.

The initially thick soliton with an amplitude of 17.5 m almost immediately (5 km after the start) generates a noticeable "step" and loses soliton shape. After the turning point (40 km), the generation of secondary solitons of positive polarity starts; the higher the amplitude of the initial soliton is, the more intense generation is. The secondary positive soliton generated from the initially thick one (Fig. 5c) also becomes thick, as was reported in [22]. The number of secondary solitons in the Gardner model is bigger than in the full-nonlinear one in all cases. Also, in all cases, the amplitude of the negative part of the pulse is higher in the full-nonlinear model, while the amplitude of secondary solitons is higher in the Gardner model.

A comparison of how amplitudes of solitons change in the analytical and numerical models is shown in Fig. 6. The propagation of the soliton with the lowest amplitude of 3.3 m (Fig. 6a) is described by the adiabatic theory for the first 20 km, half of the distance to the turning point. At large distances, a wave loses its soliton shape, as is seen in Fig. 5, where the positive "step" is seen after passing the 20-km mark. The curves corresponding to the analytical and both numerical models diverge, but both numerical models demonstrate a good fit between each other.

The soliton with the initial amplitude of 7.3 m has smaller width relative to that with the amplitude of 3.3 m (see Fig. 3) and demonstrates adiabatic propagation to the distance of 15 km (Fig. 6b), or one-third of the way to the turning point. After this, curves diverge, but, analogously to the first case, both numerical models demonstrate a good fit between each other in how the wave amplitude depends on the distance to the turning point. It can be stated that the scenario of pulse change in this case, implying moderate amplitude and being implemented in the full-nonlinear

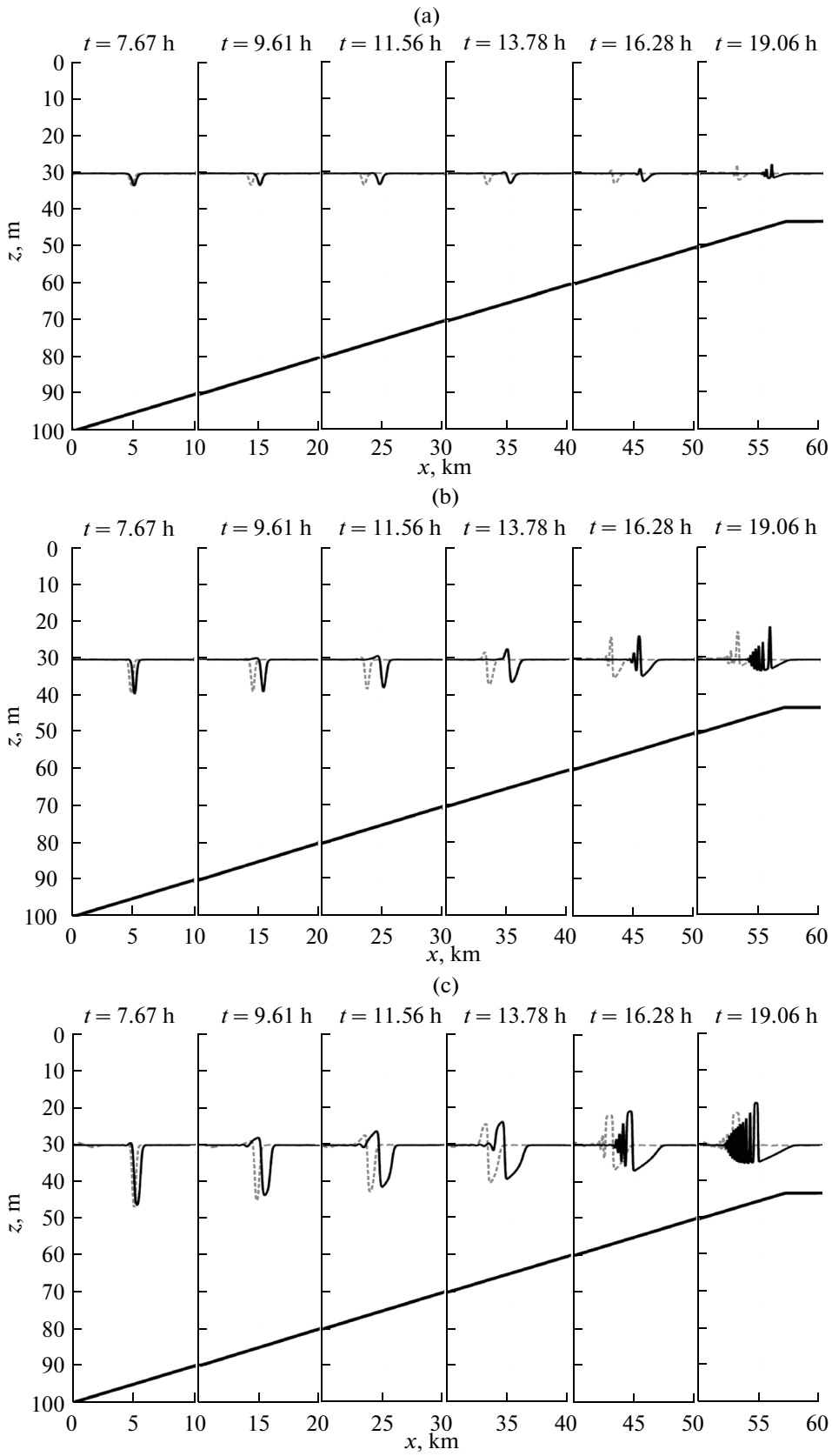

Fig. 5. Transformation of the soliton with the initial amplitudes of 3.3 (a), 9.7 (b), and 17.5 m (c) in terms of full-nonlinear (dashed line) and the Gardner (solid line) models when passing the point of zero quadratic nonlinearity.

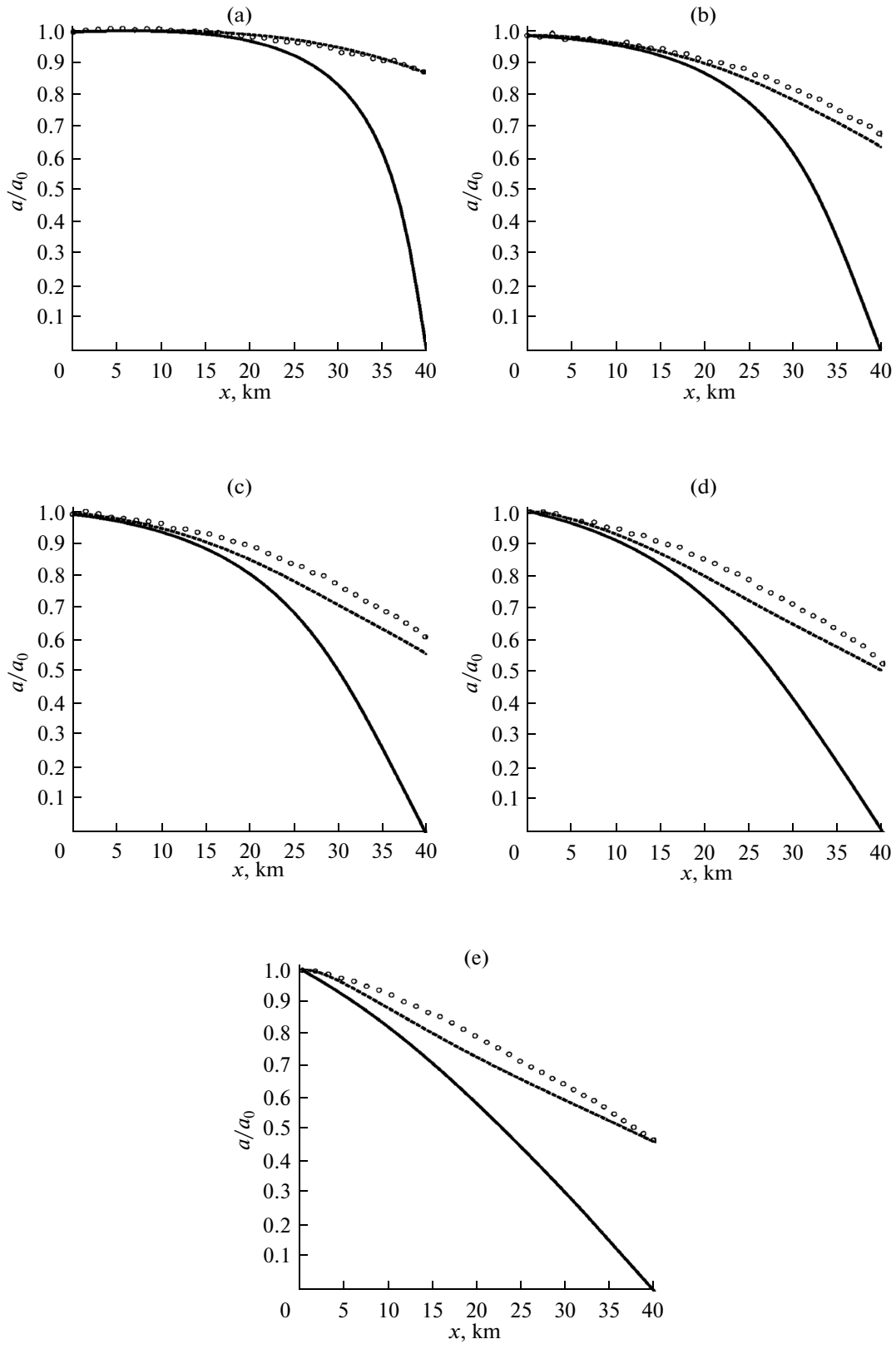

Fig. 6. Change in amplitude of propagating soliton normalized to the initial amplitude $a_0 = 3.3$ (a), 7.3 (b), 9.7 (c), 12.9 (d), and 17.5 m (e) with distance to the turning point. The adiabatic theory domain is indicated with a solid line, full-nonlinear model is shown by a pointed line, and the Gardner model is shown by a dashed line.

model, fits the Gardner approximate model very well, as was reported earlier in [30–32].

Soliton with the amplitude of 9.7 m (Fig. 6c) is the narrowest of all of them. It seems that the narrowest pulse is to propagate in accord with the adiabatic theory to bigger distances; however, the modeling results show its propagation to a distance as small as 12–13 km. The pulse shape significantly differs from the soliton one (see Fig. 5c). The numerical models begin to diverge here, beginning from a distance of 20 km, and the amplitude of the wave in the full-nonlinear model exceeds that in the Gardner model in the respective points. Note that difference between the models is 5–7%, but the curves converge again by the turning point.

Soliton with an initial amplitude of 12.9 m (Fig. 6d) propagates adiabatically only the first 5 km. At a distance of 7–8 km, the numerical models begin to diverge and, analogously to the previous case, the Gardner model gives smaller values of the negative part of the wave in the respective points relative to the full-nonlinear one. The difference between these models is no more than 7%, and the curves nearly converge again by the turning point.

Finally, soliton with the initial amplitude of 17.5 m differs from the soliton shape as soon as the start of the path and leaves the adiabatic patter of propagation at a distance of 5 km (Fig. 6e). At a distance of 10 km, numerical curves begin to diverge and they converge again by the turning point, like in the previous case.

Thus, even far from the turning points, where the coefficient of quadratic nonlinearity changes its sign, and at a quite gentle change in depth, the adiabatic propagation of soliton takes place only in the very limited zone, whose size sharply falls as the soliton shape approaches a thick soliton. This is explained by the presence of two characteristic scales in the Gardner soliton: a kink scale, which represents the forefront and back of the soliton, and the width of the soliton proper, which is the distance between kinks. The dynamics of thick solitons is considered in detail from the viewpoint of kink theory in [33–35]. In the smoothly inhomogeneous medium, a soliton can exist and be described by one formula if the distance between kinks tends to zero and their velocities are equal. In this case, the soliton is nowhere near a thick soliton. As amplitude grows, the soliton in the inhomogeneous medium loses its integrity and its transformation is the transformation of each particular kink. This process is described well in [27]. In this case, the adiabatic theory for the transformation of soliton as a single pulse is inapplicable.

CONCLUSIONS

Thus, in terms of three models—adiabatic, Gardner, and full-nonlinear—transformations of internal wave solitons of different amplitudes in a basin with a sloped bottom and two-layer stratification have been compared. It has been found that the adiabatic propagation of soliton takes place in the limited zone. The higher the amplitude of the initial soliton is, the faster the soliton loses its soliton shape and generates a "step" of an opposite polarity. As the amplitude approaches the limiting one, soliton in the inhomogeneous medium loses its integrity and its fronts (kinks) possess their own dynamics. In this case, the adiabatic theory becomes inapplicable and the pulse loses its soliton shape.

APPENDIX

The system of full Euler equations describing the motion of nonviscous incompressible stratified liquid in the vertical plane, in a Boussinesq approximation, is solved numerically:

$$\mathbf{U}_t + \mathbf{U}\nabla\mathbf{U} = -\nabla p - \rho g\mathbf{k},$$
$$\rho_t + \mathbf{U}\nabla\rho = 0,$$
$$\nabla\mathbf{U} = 0,$$
$$\rho = \frac{\rho_f - \rho_0}{\rho_0}.$$

The system is solved in 2D space (i.e., all physical values are functions of x, z, and t). Here, $\mathbf{U} = (u, w)$ is the velocity vector, u is the velocity along the horizontal x axis, w is the velocity along the vertical z axis, t is the time, ρ_f is the seawater density, ρ_0 is the constant characteristic density (in Boussinesq approximation, $\rho_f = \rho_0(1 + \rho)$), ρ is the dimensionless correction to density, and g is the free fall acceleration.

In the spatial sense, the computational domain has length L and height H. The bottom is described by function $z = h(x)$, with H being the biggest depth of the basin. The right and left boundaries are open. At the ocean surface, the "solid top" approximation is used: $w = 0$ at $z = 0$. The boundary condition at the bottom is set as impermeability condition $v_n = 0$ at $z = -H$, where v_n is the velocity along the normal to the surface. The procedure of numerical solution of the system is based on an implicit predictor–corrector two-stem finite difference scheme.

The density field in the initial time moment is initialized in accord with the following expression:

$$\rho(x, z, t = 0) = \rho_{\text{mean}}(z - \eta(x, z, t)),$$

where $\rho_{mean}(z) = -0.005\tanh\left(\frac{z + z^*}{4}\right)$, $\eta(x, z, t = 0) = F(x)\Phi(z)$; z^* is the picnocline depth; $\Phi(z)$ is the solution of boundary problem for vertical structure of mode. Horizontal disturbance $F(x)$ was set as Gardner soliton (4) with the desired parameters. The horizontal and vertical velocity components were set as follows:

$$u(x, z, t = 0) = cF(x)\frac{d\Phi}{dz}, \quad w(x, z, t = 0) = -c\Phi(z)\frac{dF}{dx}.$$

The bottom topography was also set: $h(x) = 0.001x$. The model parameters are as follows: vertical step is

1 m, horizontal step is 28 m, and time step is 2 s. For the model with the chosen parameters, the Courant–Friedrichs–Lewy stability criterion is satisfied.

A study of nonlinear dynamics in terms of Gardner equation (1) was made using numerical integration on the basis of an implicit pseudospectral scheme [36], implying the control of preservation for mass (2) and energy (3) integrals; this model has been repeatedly used by us to solve similar problems [29, 37–42]. The spatial interval was chosen proceeding from the supposed velocity of disturbances and evolutionary time and was expanded when necessary. The numerical scheme was tested on the accurate solitons of the Gardner equation with constant coefficients; additionally, the results were compared to those obtained at a double number of resolution points.

ACKNOWLEDGMENTS

This work was supported by the Federal Special-Purpose Program "Scientific-Pedagogical Personnel of an Innovative Russia 2009–2013" (project no. 14.V37.21.0611), by the Russian Foundation for Basic Research (projects nos. 12-05-00472, 13-05-90424_Ukr_f_a, and 13-05-97037_R_Povolzhye), and by the Scientific Foundation of Higher School of Economics National Research University (project no. 12-01-0103).

REFERENCES

1. F. Salusti, A. Lascaratos, and K. Nittis, "Changes of polarity in marine internal waves: Field evidence in eastern Mediterranean Sea," Ocean Modell. **82**, 10–11 (1989).
2. P. Holloway, E. Pelinovsky, T. Talipova, and B. Barnes, "A nonlinear model of the internal tide transformation on the Australian North West Shelf," J. Phys. Oceanogr. **27**, 871–896 (1997).
3. T. F. Duda, J. F. Lynch, J. D. Irish, R. C. Beardsley, S. R. Ramp, C.-S. Chiu, T. Y. Tang, and Y.-J. Yang, "Internal tide and nonlinear internal wave behavior at the continental slope in the northern South China Sea," IEEE J. Oceanic Eng. **29**, 1105–1130 (2004).
4. M.-K. Hsu, A. K. Liu, and C. Liu, "A study of internal waves in the China Seas and Yellow Sea using SAR," Cont. Shelf Res. **20**, 389–410 (2000).
5. A. K. Liu, Y. S. Chang, M.-K. Hsu, and N. K. Liang, "Evolution of nonlinear internal waves in the East and South China Seas," J. Geophys. Res. **103**, 7995–8008 (1998).
6. M. H. Orr and P. C. Mignerey, "Nonlinear internal waves in the South China Sea: Observation of the conversion of depression internal waves to elevation internal waves," J. Geophys. Res. **108** (C3), 3064 (2003).
7. S. R. Ramp, T. Y. Tang, T. F. Duda, J. F. Lynch, A. K. Liu, C.-S. Chiu, F. L. Bahr, H.-R. Kim, and Y.-J. Yang, "Internal solitons in the northeastern South China Sea. Part 1: Sources and deep water propagation," IEEE J. Oceanic Eng. **29**, 1157–1181 (2004).
8. Y.-J. Yang, T. Y. Tang, M. H. Chang, A. K. Liu, M.-K. Hsu, and S. R. Ramp, "Solitons northeast of Tung-Sha Island during the ASIAEX pilot studies," IEEE J. Oceanic Eng. **29**, 1182–1199 (2004).
9. Zh. Zhao, V. Klemas, Q. Zheng, X. Li, and X.-H. Yan, "Satellite observation of internal solitary waves converting polarity," Geophys. Res. Lett. **30**, 1988 (2003).
10. Zh. Zhao, V. Klemas, Q. Zheng, X. Li, and X.-H. Yan, "Estimating parameters of a two-layer stratified ocean from polarity conversion of internal solitary waves observed in satellite SAR images," Remote Sens. Environ. **92**, 276287 (2004).
11. Q. Zheng, V. Klemas, Q. Zheng, and X.-H. Yan, "Satellite observation of internal solitary waves converting polarity," Geophys. Res. Lett. **30** (19), 1–4 (2003).
12. E. L. Shroyer, J. N. Moum, and J. D. Nash, "Observations of polarity reversal in shoaling nonlinear internal waves," J. Phys. Oceanogr. **39**, 691–701 (2009).
13. E. L. Shroyer, J. N. Moum, and J. D. Nash, "Energy transformations and dissipation of nonlinear internal waves over New Jersey's continental shelf," Nonlinear Processes Geophys. **17**, 345–360 (2010).
14. D. Bourgault, M. D. Blokhina, R. Mirshak, and D. E. Kelley, "Evolution of a shoaling internal solitary wavetrain," Geophys. Res. Lett. **34**, L03601 (2007).
15. A. N. Serebryany and H. P. Pao, "Transition of a nonlinear internal wave through an overturning point on a shelf," Dokl. Earth Sci. **420** (4), 714–719 (2008).
16. P. Holloway, E. Pelinovsky, and T. Talipova, "A generalised Korteweg–De Vries model of internal tide transformation in the coastal zone," J. Geophys. Res. **104**, 18333–18350 (1999).
17. R. Grimshaw, E. Pelinovsky, T. Talipova, and A. Kurkin, "Simulation of the transformation of internal solitary waves on oceanic shelves," J. Phys. Oceanogr. **34**, 2774–2779 (2004).
18. R. Grimshaw, E. Pelinovsky, and T. Talipova, "Modeling internal solitary waves in the coastal ocean," Surveys in Geophysics **28**, 273–298 (2007).
19. V. Vlasenko and N. Stashchuk, "Three-dimensional shoaling of large amplitude internal waves," J. Geophys. Res. **112**, C11018 (2007).
20. V. Vlasenko and K. Hutter, "Transformation and disintegration of strongly nonlinear internal waves by topography in stratified lakes," Ann. Geophys. **20**, 2087–2103 (2002).
21. R. Grimshaw, E. Pelinovsky, and T. Talipova, "Solitary wave transformation due to a change in polarity," Stud. Appl. Math. **101**, 357–388 (1998).
22. R. Grimshaw, E. Pelinovsky, and T. Talipova, "Solitary wave transformation in a medium with sign-variable quadratic nonlinearity and cubic nonlinearity," Phys. D (Amsterdam, Neth.) **132**, 40–62 (1999).
23. R. Grimshaw, E. Pelinovsky, Y. Stepanyants, and T. Talipova, "Modelling internal solitary waves on the Australian North West Shelf," Mar. Freshwater Res. **57**, 265–272 (2006).
24. V. I. Vlasenko, L. A. Ostrovsky, and K. Hutter, "Adiabatic behaviour of strongly nonlinear internal solitary waves in slope-shelf areas," J. Geophys. Res. **110**, C04006 (2005).

25. C. J. Knickerbocker and A. C. Newell, "Internal solitary waves near a turning point," Phys. Lett. A **75A**, 326–330 (1978).

26. T. G. Talipova, E. N. Pelinovskii, and R. Grimshaw, "Transformation of a soliton through a point of zero nonlinearity," JETP Lett. **65** (1), 120–125 (1997).

27. O. Nakoulima, N. Zahibo, E. Pelinovsky, T. Talipova, A. Slunyaev, and A. Kurkin, "Analytical and numerical studies of the variable-coefficient Gardner equation," Appl. Math. Comput. **152**, 449–471 (2004).

28. T. G. Talipova, E. N. Pelinovsky, K. Lamb, R. Grimshaw, and P. Holloway, "Correlation of regional geochemical zonality of granitoid magmatism and structure of the lithosphere: Evidence from the Mongolian–Okhotsk Zone," **365** (2), 241–245 (1999).

29. R. Grimshaw, T. Talipova, E. Pelinovsky, and O. Kurkina, "Internal solitary waves: Propagation, deformation and disintegration," Nonlinear Processes Geophys. **17** (6), 633–649 (2010).

30. V. Maderich, T. Talipova, R. Grimshaw, E. Pelinovsky, B. H. Choi, I. Brovchenko, K. Terletska, and D. C. Kim, "The transformation of an interfacial solitary wave of elevation at a bottom step," Nonlinear Processes Geophys. **16** (1), 33–42 (2009).

31. V. Maderich, T. Talipova, R. Grimshaw, E. Pelinovsky, B. H. Choi, I. Brovchenko, and K. Terletska, "Interaction of a large amplitude interfacial solitary wave of depression with a bottom step," Phys. Fluids **22**, 076602 (2010).

32. T. Talipova, K. Terletska, V. Maderich, I. Brovchenko, K. T. Jung, E. Pelinovsky, and R. Grimshaw, "Internal solitary wave transformation over the bottom step: Loss of energy," Phys. Fluids **25**, 032110 (2013).

33. K. A. Gorshkov and I. A. Soustova, "Interaction of solitons as composite structures in the Gardner model," Izv. Vyssh. Uchebn. Zaved., Radiofiz. **44** (5–6), 502 (2001).

34. K. A. Gorshkov, L. A. Ostrovsky, I. A. Soustova, and V. G. Irisov, "Perturbation theory for kinks and application for multisoliton interactions in hydrodynamics," Phys. Rev. E **69**, 1–10 (2004).

35. K. A. Gorshkov, I. A. Soustova, A. V. Ermoshkin, and N. V. Zaitseva, "Approximation of the nonquasistationary evolution of nearly limiting internal-wave solitons using the Gardner equation with variable coefficients," Fund. Prikl. Gidrofiz. **6** (3), 54–62 (2013).

36. B. Fornberg, *A Practical Guide to Pseudospectral Methods* (Cambridge University Press, Cambridge, 1998).

37. A. A. Kurkin and O. E. Polukhina, "Chislennye eksperimenty po rasprostraneniyu voln Rossbi v okeane," Izv. Akad. Inzh. Nauk Ross. Fed.: Prikl. Mat. Mekh. **4**, 99–116 (2003).

38. A. A. Kurkin and O. E. Polukhina, "Nonlinear focusing of anomalous Rossby waves in the ocean: Numerical experiments," Izv., Atmos. Ocean. Phys. **41** (1), 93–101 (2005).

39. O. E. Polukhina and N. M. Samarina, "Cylindrical divergence of solitary internal waves in the context of the generalized Gardner equation," Izv., Atmos. Ocean. Phys. **43** (6), 755–761 (2007).

40. E. Pelinovsky, O. Polukhina, A. Slunyaev, and T. Talipova, "Internal solitary waves," in *Solitary Waves in Fluids* (WIT Press, Boston, 2007), Chap. 4, pp. 85–110.

41. O. E. Kurkina, A. A. Kurkin, T. Soomere, E. N. Pelinovsky, and E. A. Rouvinskaya, "Higher-order (2+4) Korteweg–De Vries-like equation for interfacial waves in a symmetric three-layer fluid," Phys. Fluids **23** (11), 116602-1–13 (2011).

42. O. E. Kurkina, A. A. Kurkin, E. A. Ruvinskaya, E. N. Pelinovsky, and T. Soomere, "Dynamics of solitons in a nonintegrable version of the modified Korteweg–de Vries equation," JETP Lett. **95** (2), 91–95 (2012).

Translated by N. Astafiev